# Generating Artificial Sensations with Spinal Cord Stimulation in Primates and Rodents

Amol P. Yadav[1-4], Shuangyan Li[3,11,12], Max O. Krucoff[1,8], Mikhail A. Lebedev[2,9,10], Muhammad M. Abd-El-Barr[1], Miguel A.L. Nicolelis[1-7]

[1]Department of Neurosurgery, [2]Center for Neuroengineering, [3]Department of Neurobiology, [4]Department of Biomedical Engineering, [5]Department of Psychology and Neuroscience, [6]Department of Neurology, Duke University, Durham, NC 27710, [7]Edmond and Lily Safra International Institute of Neuroscience, Natal, Brazil 59066060, [8]Department of Neurosurgery, Medical College of Wisconsin, Milwaukee, WI 53226, [9]Center for Bioelectric Interfaces of the Institute for Cognitive Neuroscience, National Research University Higher School of Economics, Moscow, Russia 101000, [10]Department of Information and Internet Technologies of Digital Health Institute, I.M. Sechenov First Moscow State Medical University, Moscow, Russia 119146, [11]State Key Laboratory of Reliability and Intelligence of Electrical Equipment, School of Electrical Engineering, [12]Tianjin Key Laboratory Bioelectromagnetic Technology and Intelligent Health, Hebei University of Technology, Tianjin 300130, P.R.China

Corresponding Author:

Amol P. Yadav, Ph.D.
Department of Neurosurgery
Duke University,
Box 103905, Durham, NC 27710
amol.yadav@duke.edu

**Abstract**

For patients who have lost sensory function due to a neurological injury such as spinal cord injury (SCI), stroke, or amputation, spinal cord stimulation (SCS) may provide a mechanism for restoring somatic sensations via an intuitive, non-visual pathway. Inspired by this vision, here we trained rhesus monkeys and rats to detect and discriminate patterns of epidural SCS. Thereafter, we constructed psychometric curves describing the relationship between different SCS parameters and the animal's ability to detect SCS and/or changes in its characteristics. We found that the stimulus detection threshold decreased with higher frequency, longer pulse-width, and increasing duration of SCS. Moreover, we found that monkeys were able to discriminate temporally- and spatially-varying patterns (i.e. variations in frequency and location) of SCS delivered through multiple electrodes. Additionally, sensory discrimination of SCS-induced sensations in rats obeyed Weber's law of just noticeable differences. These findings suggest that by varying SCS intensity, temporal pattern, and location different sensory experiences can be evoked. As such, we posit that SCS can provide intuitive sensory feedback in neuroprosthetic devices.

## Main

Lack of sensory feedback from a brain-controlled actuator or prosthetic device is a major hindrance to successful integration of the neuroprosthesis in activities of daily life and rehabilitative protocols (1-3). The somatosensory cortex (S1) and thalamus have been proposed as potential targets for neurostimulation that could produce naturalistic somatosensory percepts (4-10). However, stimulating these brain areas requires surgical implantation of deep intracranial electrodes – a procedure associated with significant risks. While peripheral nerve stimulation provides a less invasive alternative, sensations evoked with this method are highly localized, and thus limited in their applicability as a general-purpose sensory input pathway to the brain (11-13). Previously, our group demonstrated that electrical stimulation of the dorsal surface of the spinal cord can be used to transmit sensory information to the brain or between multiple brains in rodents (14). Building on this previous work, here we explored whether rats and nonhuman primates can learn to detect and discriminate artificial sensations generated with dorsal thoracic epidural spinal cord stimulation (SCS). Understanding the psychophysical relationship between SCS parameters and the ability to detect sensations is critical for the development of novel neuroprosthetic devices that restore function to people with sensory disabilities. We examined how sensory discrimination changes when SCS parameters are varied in both rodent and primate models, and we asked whether animals can learn to discriminate sensations generated by SCS patterns that vary in frequency and spatial location. After training the animals to discriminate SCS patterns, we determined whether artificial sensations evoked by SCS of variable frequency follow Weber's law of just noticeable differences (JND) - a critical property defining sensory discrimination.

## Results

We implanted three rhesus monkeys with percutaneous epidural SCS electrodes at the dorsal thoracic spinal level and trained them to perform a two-alternative forced choice task (2AFC) using a joystick-controlled cursor (Figure 1a, Supplementary Figures 1b, 1c, and 1d). In a typical

**Figure 1**

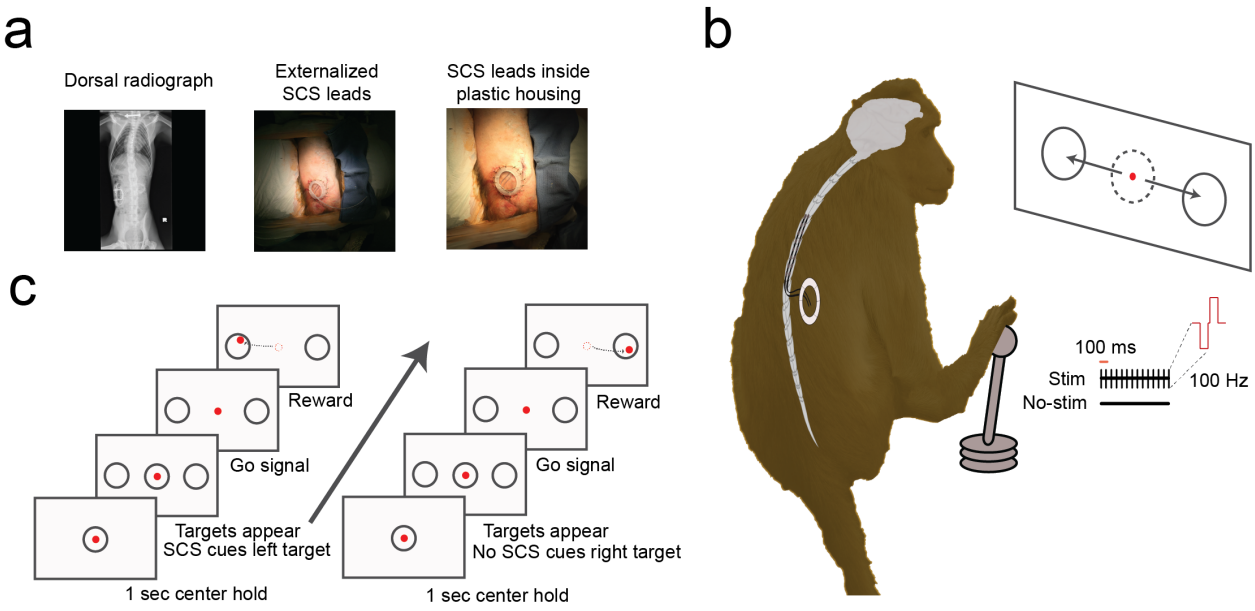


Figure 1: Surgery and experimental task setup. a) We implanted three non-human primates (rhesus monkeys) with SCS percutaneous leads over the T6-T10 dorsal epidural surface of the spinal cord. Leads were externalized from the lower back area and secured inside a custom plastic housing. Leads were manually accessed by the experimenter for daily training and connected to a custom pulse stimulator. b) Monkeys were seated in a primate chair in front of a computer monitor with access to a hand-controlled joystick. They participated in a two-alternative forced choice task (2AFC) by moving the joystick controlling a cursor on the screen in order to receive a juice reward. c) On each trial, monkeys had to hold the cursor inside the center circle for 1 sec. After that, targets appeared on the left and right side of the center. Monkeys were presented with 'SCS-ON' (biphasic, 100 Hz, 200 μs, 1 sec) cue or 'SCS-OFF' cue when the targets appeared. After a brief, variable hold period (100-1000 ms), the center circle disappeared which indicated them to move the joystick. Monkeys had to move the cursor inside the left target on 'SCS-ON' trials and inside the right target on 'SCS-OFF' trials. Correct response resulted in juice reward. In the SCS discrimination task, stimulation was delivered at 200 μs for 1 sec. Monkeys had to select left target for 100 Hz stimulus and right target for 200 Hz stimulus in the frequency discrimination task. For spatial discrimination task, monkeys had to choose left target when stimulation was delivered at electrode pair 1 and right target for stimulation at electrode pair 2.

experimental session, a monkey was seated in a chair in front of a monitor that displayed task-related cues. The animals moved a hand-held joystick to control a cursor on a screen (Figure 1b).

A typical trial consisted of a brief (300 - 500 ms) center hold period after which two targets appeared. After a brief preparatory period (250 – 1000 ms) during which a trial cue was presented, the monkeys had to move the cursor into one of the targets to obtain a juice reward. Monkeys were initially trained to identify the correct target using a visual cue; however, during the experimental sessions, no visual cues were presented, and they selected a target by interpreting SCS cues alone. In the detection task, monkeys had to select the left target if SCS was delivered during the preparatory period and right target if no SCS was delivered (Figure 1c). In the discrimination task, monkeys had to select the left target for the 100 Hz stimuli and right target for the 200 Hz stimuli (frequency discrimination) and the left target for electrode pair 1 and right target for electrode pair 2 (spatial discrimination).

*Monkeys learned to detect SCS stimuli*

Monkeys M, O, and K learned to detect SCS-induced sensory percepts evoked using percutaneous dorsal thoracic epidural electrodes (T7 for monkey M, T5-T6 for monkey O, T5-T6 for monkey K). Performance of all monkeys started below chance levels of 50% and reached above 90% after learning (Figure 2a). Monkey M started detection performance at 49% and reached a maximum of 93% in 16 days; monkey O started at 49% and reached a maximum of 97% in 10 days; and monkey K started at 41% and reached a maximum of 90% in 8 days.

*Electrode thresholds and electrode mapping*

Once the monkeys learned to detect SCS sensations, we used psychometric analysis to determine the detection thresholds for different electrode combinations (Figure 2b). We observed that the detection thresholds varied from 315.6 μA to 340 μA for monkey O and 197 μA to 748 μA for monkey K for different cathode-anode electrode pairs (Figure 2c, right). Once electrode

**Figure 2**

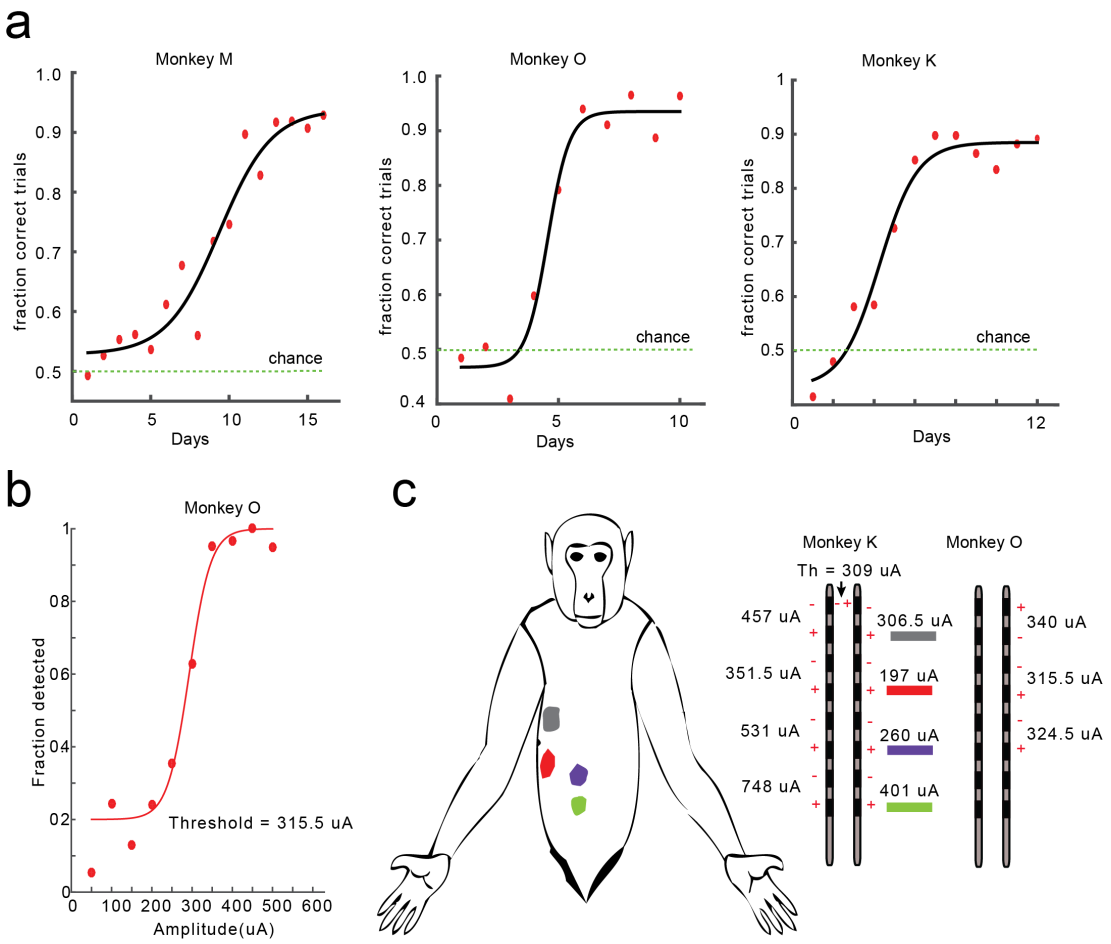


Figure 2: Monkeys learned to detect SCS stimuli. a) Learning curves (sigmoidal fits) for monkeys M, O, and K showing behavioral performance (fraction correct trials) as a function of training days. b) Psychometric function showing fraction trials detected as a function of stimulation amplitude in monkey O. Detection threshold is defined as amplitude at which monkeys achieved 75% performance on detection task. c) Mapping of bipolar electrode pairs on monkey K's body where stimulation on right-side electrode at suprathreshold amplitude elicited minor muscle twitches or skin flutter (color coded by electrode pairs and corresponding sensory thresholds shown on right). Monkey body shape is adapted from (15).

thresholds were determined, we mapped the bipolar electrode pairs to locations on the monkey's body by stimulating at suprathreshold amplitudes and observing stimulation-induced minor

127 muscle twitches or skin flutter. We observed that muscle twitches/skin flutter were elicited in the
128 trunk and abdomen area only at suprathreshold values but not at sensory threshold values (Figure
129 2c). We also noted that in both monkeys K and O experimentally determined sensory thresholds
130 were always lower than the observed motor thresholds for each cathode-anode electrode pair
131 (Supplementary Figure 3b).

132 *Sensitivity to detection of sensory percepts in primates*

133 Thereafter, we investigated the psychophysical relationship between stimulation parameters and
134 detection of sensory percepts by varying stimulation amplitudes along with stimulation frequency,
135 pulse-width, or duration of stimulation while keeping the other two parameters constant.

136 We varied amplitude from 50 μA to 800 μA for pulse-widths of 50 μs, 100 μs, 200 μs, and 400 μs
137 for monkey K, and pulse-widths of 100 μs, 200 μs, and 400 μs for monkey O. Frequency and
138 duration of stimulation were held constant (Figures 3a, 3e, and Supplementary Figure 2a). We
139 observed that stimulus detection threshold significantly decreased with increasing stimulation
140 pulse-width ($p<0.05$, repeated measures one-way ANOVA) for both animals (Figure 3h).

141 We varied amplitude from 50 μA to 800 μA for frequencies of 10 Hz, 20 Hz, 50 Hz, 100 Hz, 200
142 Hz, and 500 Hz for monkey K, and frequencies of 20 Hz, 50 Hz, 100 Hz, 200 Hz, and 500 Hz for
143 monkey O while keeping pulse-width and duration of stimulation constant (Figures 3b, 3f, and
144 Supplementary Figure 2b). We observed that stimulation detection threshold significantly
145 decreased with increasing stimulation frequency ($p<0.05$, repeated measures one-way ANOVA)
146 for both animals (Figure 3i).

147 We varied amplitude from 50 μA to 600 μA for duration of 50 ms, 100 ms, 500 ms, and 1000 ms
148 for monkey K, and amplitude between 50 μA to 700 μA for duration of 50 ms, 100 ms, and 500
149 ms for monkey O, while keeping pulse-width and frequency of stimulation constant (Figures 3c,
150 3g, and Supplementary Figure 2c). We observed that stimulation detection threshold significantly

**Figure 3**

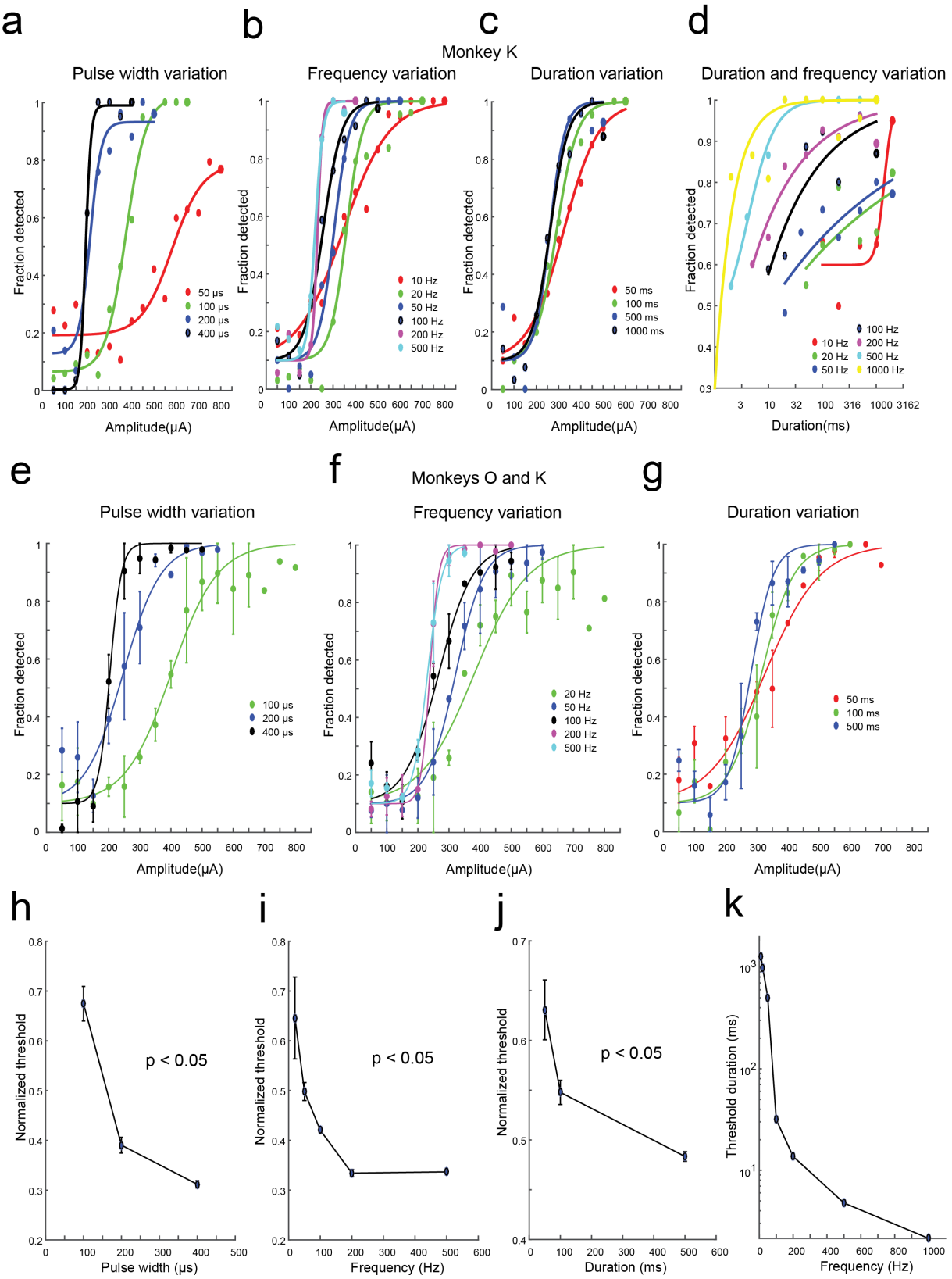
a
b
c
d
Monkey K
Pulse width variation
Frequency variation
Duration variation
Duration and frequency variation
Fraction detected
Amplitude(μA)
Duration(ms)
50 μs
100 μs
200 μs
400 μs
10 Hz
20 Hz
50 Hz
100 Hz
200 Hz
500 Hz
50 ms
100 ms
500 ms
1000 ms
1000 Hz
e
f
g
Monkeys O and K
h
i
j
k
Normalized threshold
Threshold duration (ms)
Pulse width (μs)
Frequency (Hz)
Duration (ms)
p < 0.05

153 Figure 3: Psychophysical evaluation of SCS sensory detection with varying stimulation parameters in
154 primates. Once monkeys learned to detect SCS stimuli at the standard parameters (frequency: 100 Hz,
155 pulse width: 200 μs, duration: 1 sec), we allocated different blocks of sessions where (pulse width &
156 amplitude; panels 'a' and 'e'); (frequency & amplitude; panels 'b' and 'f'); and (duration & amplitude; panels
157 'c' and 'g') were varied while keeping other parameters constant. In monkey K, in a separate block,
158 frequency and duration was varied with other parameters constant (pulse width: 200 μsec and amplitude:
159 325 μA). Psychometric curves in a-g are sigmoidal fits. Panels a-d represent psychometric curves for
160 monkey K, while panels e-g represent psychometric curves fitted to data averaged across monkeys K and
161 O (circles and error bars are mean ± sem). Panels h, i, j, indicate normalized detection thresholds
162 (normalized by maximum amplitude used in the experiment block of each individual monkey) averaged
163 across both monkeys (mean ± sem). Detection threshold were calculated as 75% fraction detected at the
164 stimulation parameters shown in panels a-c (monkey K) and Supplementary Figure 2 a-c (monkey O). P-
165 values were calculated using repeated measures one-way ANOVA. Panel k shows threshold duration
166 obtained as 75% detection from curves in panel d as a function of frequency.

167

168 decreased with increasing stimulation duration ($p<0.05$, repeated measures one-way ANOVA) for
169 both animals (Figure 3j).

170 In monkey K, we varied both frequency and duration of stimulation while keeping amplitude and
171 pulse-width of stimulation constant. We observed that as the frequency of stimulation increased,
172 the duration of stimulation to reach detection threshold decreased (Figures 3d and 3k). Monkey
173 K was able to detect a sensory percept generated by merely two stimulation pulses delivered at
174 1000 Hz.

175 *Sensitivity to detection of sensory percepts in rats*

176 We have previously shown that rats learn to detect sensations generated by epidural SCS
177 delivered at the T2 spinal level (14). In order to study the psychophysical performance of rats

178 **Figure 4**

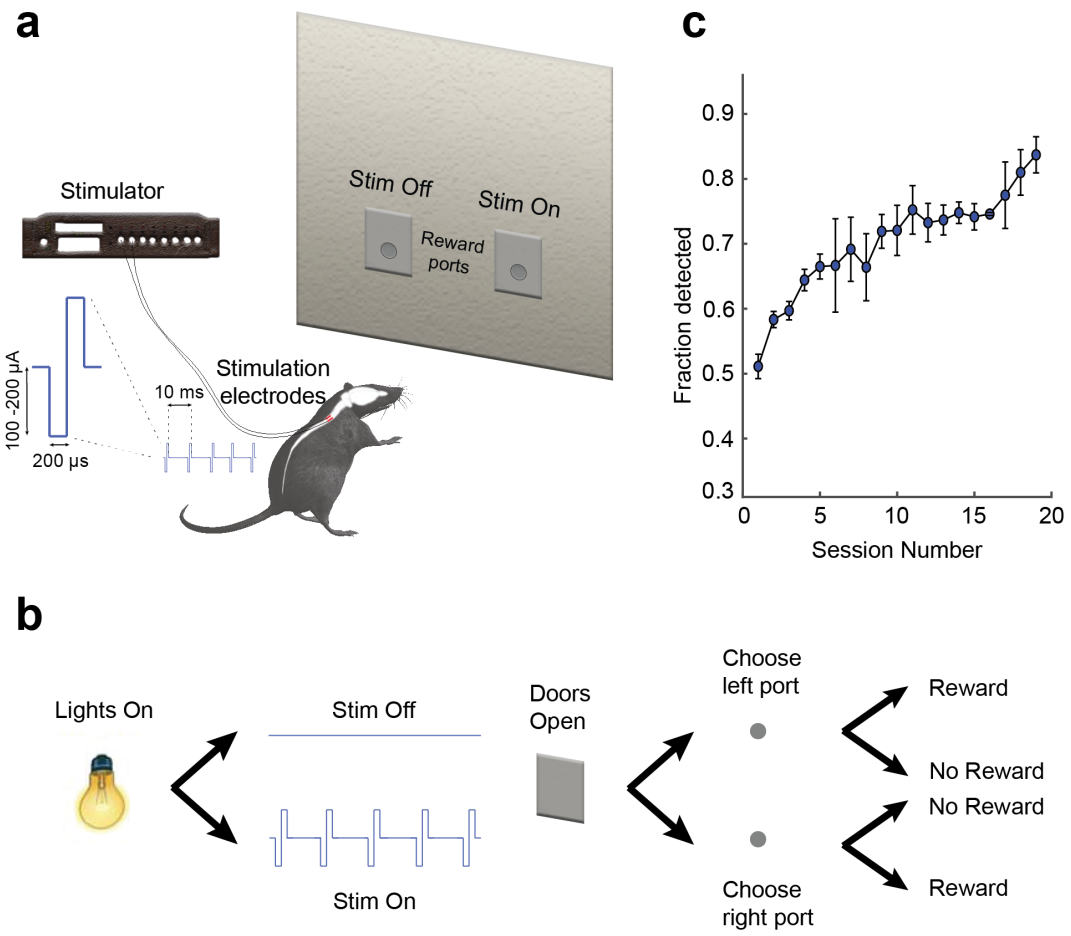


179

180 Figure 4: Behavioral task setup and rats learned to detect SCS stimuli. a) The experiment task consisted
181 of a closed behavioral chamber with two reward ports on one side of the chamber. The ports were covered
182 with vertical sliding doors. Five rats were implanted with bipolar stimulation electrodes on the dorsal surface
183 of the spinal cord at the T3 spinal level. b) Task consisted of a house light turning 'on', followed by sensory
184 cues for 1 second. During the cue period SCS was either delivered or not delivered. After the cue period
185 both reward doors opened, and the rat had to make a nose poke response in either of the ports to receive
186 water reward. If SCS was delivered rats had to poke inside the left port and if not delivered, then they had
187 to poke inside the right reward port. Poking in the correct reward poke initiated a water reward, while
188 incorrect pokes were not rewarded. c) Rats learned to detect SCS stimuli over a period of 15 – 25 days as
189 indicated – learning curve showing task performance indicated by fraction trials detected as a function of
190 training sessions. Circles and error bars indicate mean ± sem.

**Figure 5**

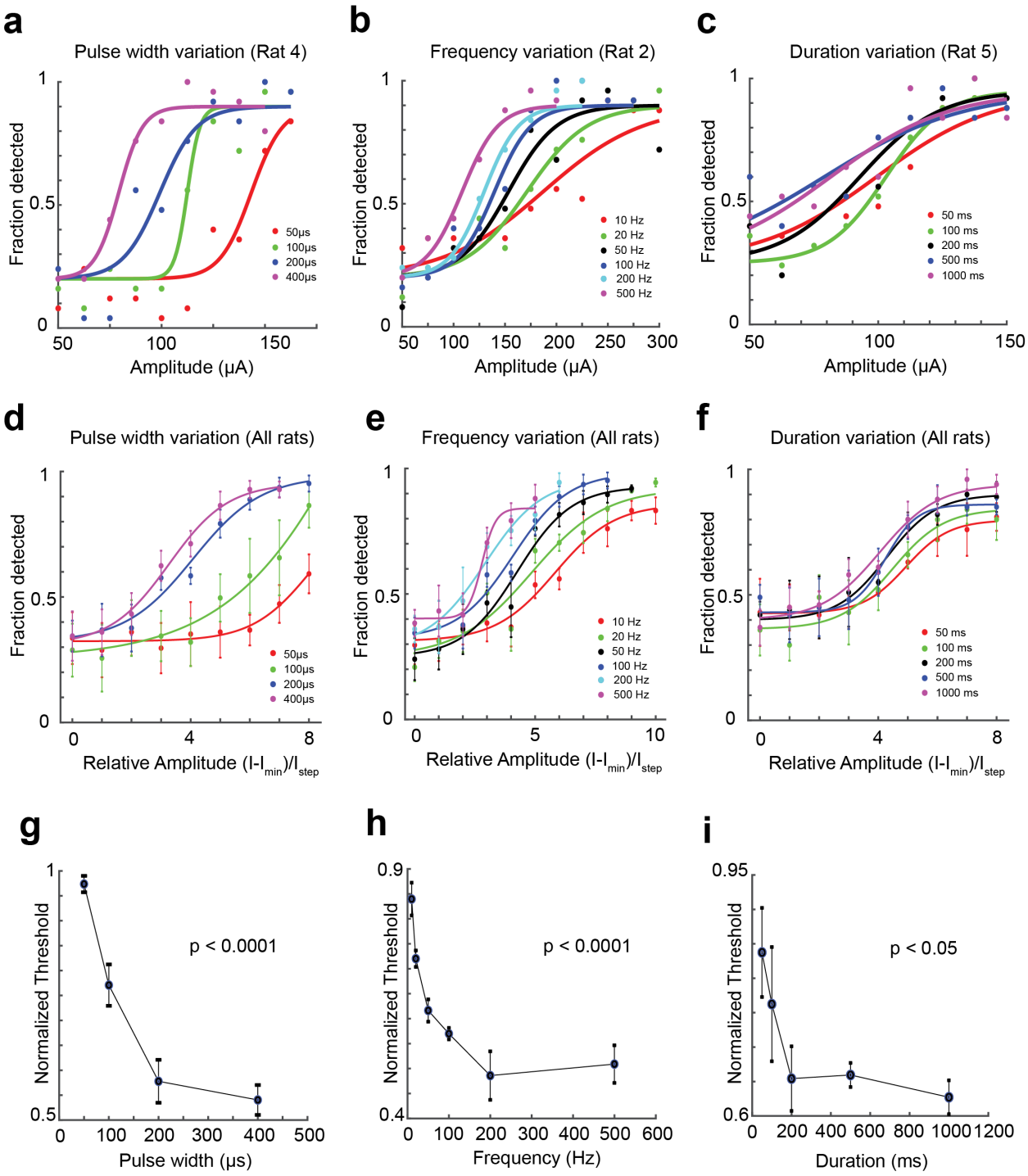


<u>Figure 5: Psychophysical evaluation of SCS sensory detection with varying stimulation parameters in rats.</u>

Once rats learned to detect SCS stimuli at the standard parameters (frequency: 100 Hz, pulse width: 200

195 μs, duration: 1 sec), we allocated different blocks of sessions where (pulse width & amplitude; panel 'a');
196 (frequency & amplitude; panel 'b'); and (duration & amplitude; panel 'c') were varied while keeping other
197 parameters constant. a, b, c) Psychometric curves from representative rats showing a leftward shift of
198 curves as the pulse-width (rat 4), frequency (rat 2), and duration (rat 5) of stimulation increased. d, e, f)
199 Psychometric curves with averaged data across five rats indicate leftward shift as pulse-width, frequency,
200 and duration are increased. X-axis represents relative amplitude values (for each rat raw amplitude values
201 were subtracted by minimum amplitude and the difference was divided by amplitude step size). Circles and
202 error bars are mean ± sem across five rats. Curves in panels 'a-f' are sigmoidal fits. Panels 'g', 'h', and 'i'
203 indicate normalized detection thresholds. Thresholds were calculated as 75% fraction detected at different
204 stimulation parameters consistent with panels 'a-f' and then normalized by maximum amplitude used in the
205 experimental block of each rat. Circles and error bars are mean ± sem across five rats. P-values were
206 calculated using repeated measures one-way ANOVA.

207

208 pertaining to sensory detection, initially we trained rats to detect SCS stimuli using a 2-AFC task
209 in a slightly modified behavioral chamber (Figure 4a and 4b). We trained five rats to detect SCS
210 stimuli delivered at the T3 spinal level (frequency: 100 Hz, pulse-width: 200 μs, duration: 1 sec,
211 biphasic pulses at 243.7±57.9 μA, Figure 4c).

212 Once rats learned the basic detection task, we varied stimulation parameters such as: pulse width
213 (50 – 400 μs); frequency (10 – 500 Hz); and duration (50 – 1000 ms) independently with
214 stimulation amplitude (Figures 5a, 5d – pulse width; 5b, 5e – frequency; and 5c, 5f – duration).
215 Similar to the results in monkeys, we observed that stimulation detection thresholds significantly
216 decreased with increasing pulse-width (Figure 5g, $p < 0.0001$, repeated measures one-way
217 ANOVA), frequency (Figure 5h, $p < 0.0001$, repeated measures one-way ANOVA) and duration
218 (Figure 5i, $p<0.05$, repeated measures one-way ANOVA) for all rats.

219

**Figure 6**

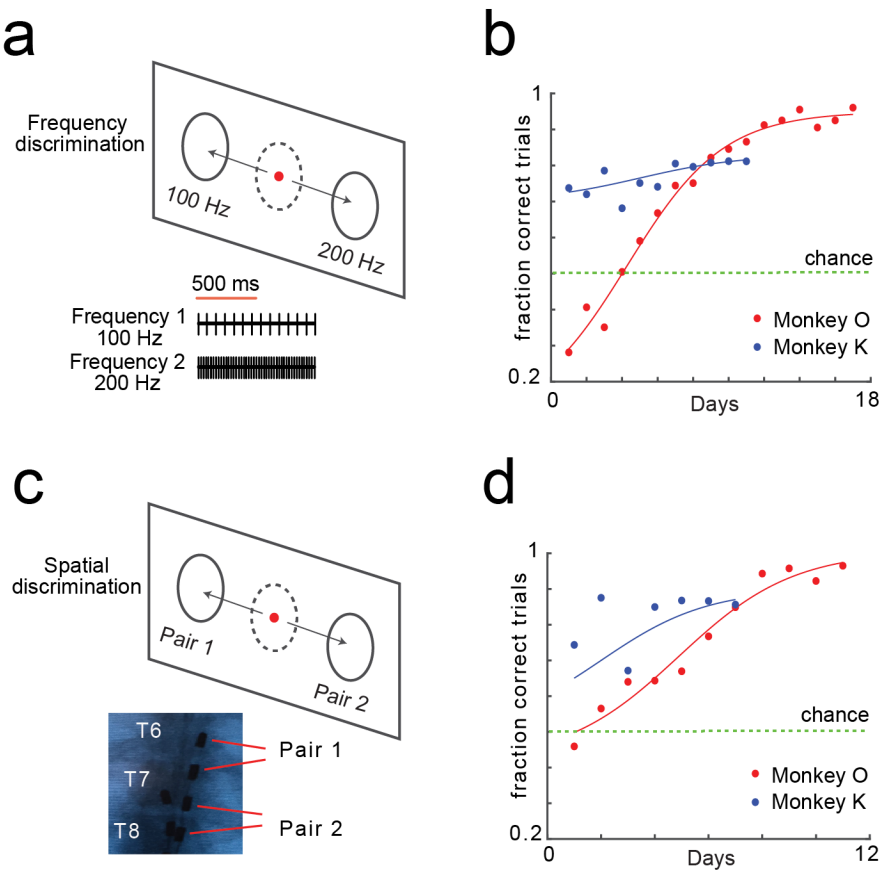


Figure 6: Monkeys learned to discriminate SCS stimuli varying in frequency and spatial location of electrodes. a,b) Monkeys K and O learned to discriminate SCS stimuli delivered at the same electrode location but varying in frequency (100 Hz vs 200 Hz). Monkey O was stimulated at same amplitude while monkey K was stimulated at the respective threshold amplitude for 100 Hz and 200 Hz. c,d) Monkeys K and O learned to discriminate stimulation delivered at electrode pair 1 (T6 - T7 spinal level) vs electrode pair 2 (T7-T8 spinal level). Curves in panels b and d indicate sigmoidal fits to fraction correct trials displayed as a function of training days.

*Sensory discrimination in primates*

We then trained monkeys K and O to discriminate SCS that varied in frequency as well as location

232 of stimulation. On frequency discrimination (100 Hz vs 200 Hz, Figure 6a), monkey O's
233 performance improved from 29% on day 1 to 96% on day 17 of training, while monkey K's
234 performance improved from 74% on day 1 to 81% on day 11 (Figure 6b). Spatial discrimination
235 was achieved by stimulating electrode pair 1 versus electrode pair 2 (Figure 6c), where monkey
236 O's performance improved from 46% on day 1 to 97% on day 11 and monkey K's performance
237 improved from 74% on day 1 to 86% on day 7 (Figure 6d).

238 *Sensory discrimination and Weber's law in rats*

239 We had previously shown that rats can learn to discriminate up to four different time-varying
240 patterns of stimulation (14). In our current work, we trained rats to discriminate SCS stimuli with
241 different frequencies using the same behavioral setup that was used for the detection task
242 (Supplementary Figure 4a). In the basic training, rats learned to discriminate between 10 Hz and
243 100 Hz of stimulation delivered at pulse-width of 200 μsec, and duration of 1 sec (Supplementary
244 Figure 4b). Thereafter, we studied whether discrimination of sensations induced by different
245 stimulation frequencies follows the rules of Weber's law (16), which states that Just-Noticeable
246 Differences (JNDs) between a standard frequency and comparison frequency should linearly
247 increase with the standard frequency of stimulation. To this end, we determined JNDs at different
248 standard frequencies (10 – 100 Hz) where the comparison frequency was higher than the
249 standard (Figure 7a). We observed that JNDs had a significant linearly increasing relationship
250 with the standard frequency of stimulation (Figure 7b, $p < 0.0001$, linear regression test). After
251 that, we kept the standard as a higher frequency value (100 – 400 Hz) and decreased the
252 comparison frequency randomly from that value (Figure 7c). In this case also, we observed that
253 the JNDs for lower frequency comparison significantly increased linearly as the standard
254 frequency increased (Figure 7d, $p < 0.0001$, linear regression test). These results suggest that the
255 JND rule defined by Weber's law holds true for sensory discrimination of SCS frequencies.

256

**Figure 7**

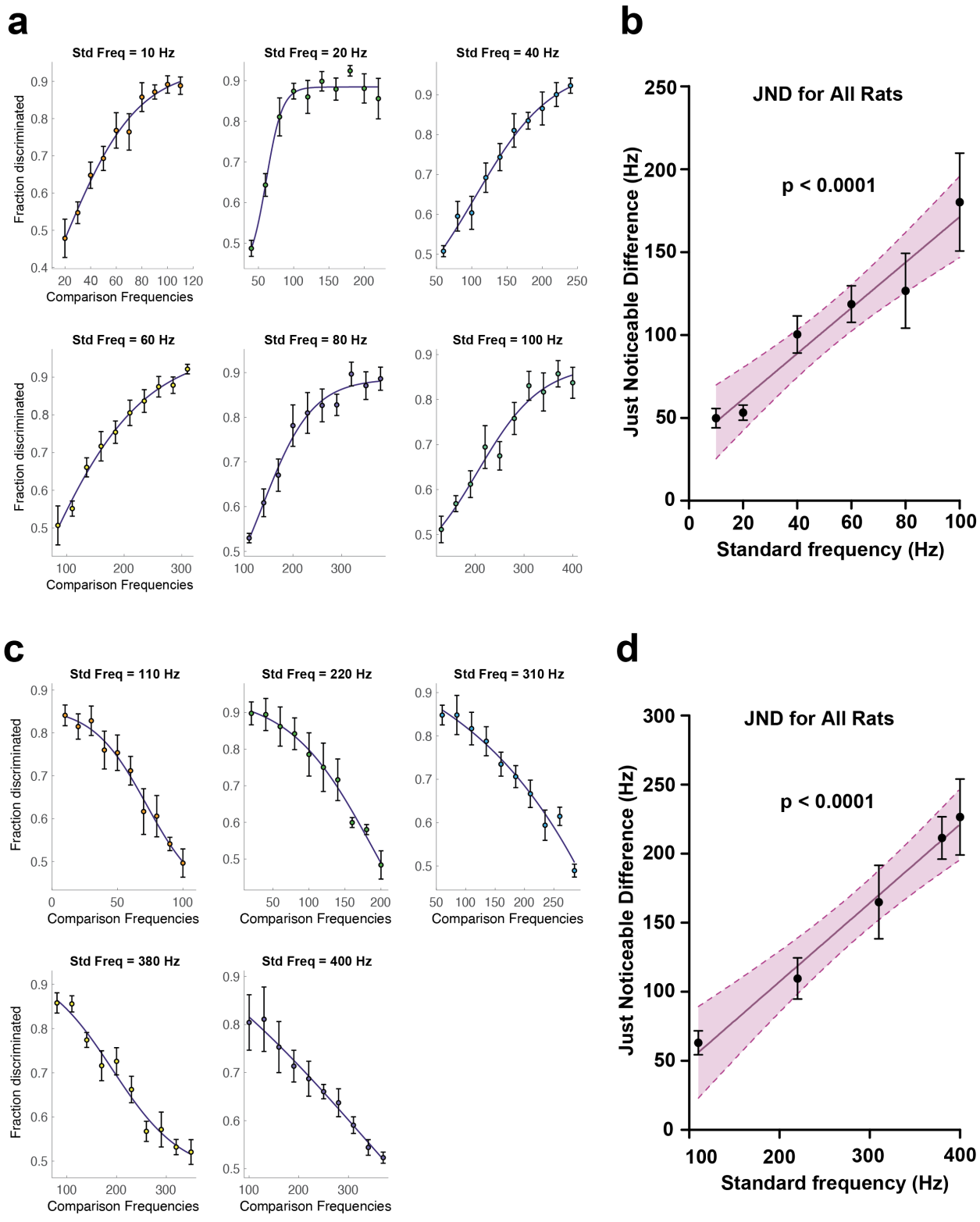
a
Std Freq = 10 Hz
Std Freq = 20 Hz
Std Freq = 40 Hz
Std Freq = 60 Hz
Std Freq = 80 Hz
Std Freq = 100 Hz
Fraction discriminated
Comparison Frequencies
b
JND for All Rats
p < 0.0001
Just Noticeable Difference (Hz)
Standard frequency (Hz)
c
Std Freq = 110 Hz
Std Freq = 220 Hz
Std Freq = 310 Hz
Std Freq = 380 Hz
Std Freq = 400 Hz
Fraction discriminated
Comparison Frequencies
d
JND for All Rats
p < 0.0001
Just Noticeable Difference (Hz)
Standard frequency (Hz)

Figure 7: Discrimination of higher and lower comparison frequency obeys Weber's Law. a) Fraction of trials correctly discriminated from standard frequency of 10 Hz, 20 Hz, 40 Hz, 60 Hz, 80 Hz, and 100 Hz, when compared to a range of higher frequency stimuli. c) Fraction of trials correctly discriminated from standard frequency of 110 Hz, 220 Hz, 310 Hz, 380 Hz, and 400 Hz, when compared to a range of lower frequency stimuli. Circles and error bars in 'a' and 'c' indicate mean ± sem. Curves indicate sigmoid fits to the data. Just noticeable difference (JND) is considered as the comparison frequency value that achieves 75 % discrimination ability. b, d) Just noticeable difference as a function of standard frequency is indicated by black circles and error bars. Black line is linear regression fit to the data and pink bounds indicate 95% confidence bound of the regression line. JNDs associated with higher frequency and lower frequency comparison were significantly linearly related with standard frequency. P-values were calculated using linear regression test.

## Discussion

In this study, we found that rhesus monkeys and rats can learn to detect and discriminate artificial sensations induced by SCS following several days of exposure. The threshold for detecting SCS decreases with increasing pulse width, frequency, and duration of the stimulus. We also documented the ability of monkeys to discriminate sensations that are generated by stimulation pulses with varying frequency and spatial location. In rats, we showed that the just-noticeable differences (JNDs) from a perceivable stimulus frequency were linearly related to the perceivable frequency when it was compared with a stimulus that had either higher or lower frequency. These results demonstrated the unique ability of SCS as a novel transmission channel to the brain to encode highly contextual sensory information.

Our results on behavioral sensitivity to detection of sensation in rodents and primates were comparable to those observed with Intracortical Microstimulation (ICMS) of S1 (5, 17). Notably, sensitivity to stimulus amplitude increased with increasing pulse width, frequency, and duration

284 of stimulation. ICMS amplitude using currently FDA-approved UTAH arrays is usually restricted
285 below ~100 μA due to the possibility of brain tissue damage, which limits the amplitude range for
286 neuroprosthetic applications between detection thresholds of 20 - 50 μA and maximum allowable
287 safe amplitude of ~100 μA. In our SCS study, detection thresholds had a wider range from 200 –
288 800 μA at different stimulation settings and all detection thresholds were consistently on the non-
289 damaging side of the boundary between damaging and non-damaging stimulation delineated by
290 Shannon equation [log(D) = k – log (Q), with k = 1.85] on log charge density versus log charge
291 per phase plot (Supplementary Figure 3a) (18). Assuming a commercially accepted maximum
292 charge density of 30 μC/cm$^2$ and minimum pulse-width of 50 μs (19), it could be estimated that
293 maximum SCS current of ~80 mA in monkeys and ~3 mA in rats could be delivered using
294 electrode contacts (monkeys: 0.1319 cm$^2$; rats: 0.005 cm$^2$) reported in our study without causing
295 tissue damage.

296 Frequency modulation has been historically considered a promising method for providing sensory
297 feedback with several studies showing that animals are capable of discriminating ICMS
298 frequencies and that frequency modulation obeys Weber's law. (4, 20-22), While ICMS amplitude
299 modulation in monkeys failed to follow Weber's law (5), experiments in rats showed that
300 modulation of perceived intensity by amplitude and pulse-width modulation followed Weber's law
301 (17). In our study, we investigated whether rats and monkeys could learn to discriminate SCS
302 frequencies. Although monkeys O and K learned to discriminate 100 Hz SCS from 200 Hz, after
303 taking a closer look at their learning curves it was evident that they displayed different learning
304 behaviors in the frequency discrimination task (Figures 6b and 6d). Monkey O started at lower
305 discrimination performance at earlier training sessions but reached higher level of performance
306 toward the end of training, whereas monkey K's performance started higher than chance and
307 improved marginally as the training progressed. These differences in learning behavior could be
308 attributed to the fact that monkey O was stimulated at constant amplitude for both frequency

values (100 Hz and 200 Hz) while monkey K was stimulated at each frequency's threshold amplitude. It is quite possible that monkey O was discriminating differences in perceived magnitudes of the sensory percepts while monkey K was discriminating differences in the qualitative nature of the percepts induced. Rats are capable of discriminating temporal patterns of SCS when the number of pulses are kept constant but the frequency of stimulus is varied (14). In addition to that, our current results indicate that JNDs associated with SCS frequency discrimination in rats clearly follow Weber's law because JNDs linearly increased with standard stimulation frequency (Figure 7b and 7d). There were at least three discriminable percepts between 10 Hz and 200 Hz. It can be argued that applying frequency modulation simultaneously with amplitude and pulse-width modulation would potentially increase the number of distinct discriminable percepts that are possible within the amplitude range allowed on current SCS electrodes. Therefore, further experiments exploring the relationship between sensory discrimination and frequency, pulse-width, amplitude, and duration of stimulation are necessary to understand how these parameters relate to perceived intensity and quality of sensation evoked by SCS.

A major advantage of SCS is its ability to target multiple dermatomes simultaneously with a single electrode array. In particular, a single, commercially available SCS lead with multiple contacts can evoke sensations in multiple dermatomes simultaneously due to the bilateral sensory representation of the entire lower body in the ascending dorsal column fibers. It is quite apparent from our results that monkeys can learn to discriminate the spatial location of the sensations evoked by SCS (Figure 6d). This suggests that we can take full advantage of the medio-lateral/rostro-caudal somatotopy represented in the dorsal column fibers in combination with spatiotemporal stimulation patterns to electrically induce targeted tactile or proprioceptive sensations in the body. This view is also supported by evidence from computational studies which indicate that epidural SCS activates dorsal column fibers up to a depth of 0.2-0.25 mm from the

334 dorsal surface (23-27). However, additional work on miniaturizing electrode contacts and accurate
335 mapping of SCS-induced sensations needs to be performed to be able to elicit precise sensations.
336 In addition, the ability of SCS to modulate neuronal activity in supraspinal brain structures is quite
337 desirable from a neuroprosthetic as well as a therapeutic application standpoint (14, 28-31). A
338 major limitation of our study is the short experimental time (Supplementary Figure 1a) we had
339 available for primates – maximum of 5 months – due to the risk of infection associated with
340 externalized SCS leads. A fully implantable stimulation system, like the one implanted in chronic
341 pain patients could potentially extend our study indefinitely and allow us to perform longer
342 experiments in monkeys. Nevertheless, in rodents we were able to perform longer post-implant
343 experiments because the electrodes and their wires were fully enclosed inside the body.

344 In conclusion, we have successfully demonstrated that SCS can be used to encode sensory
345 information in both rats and monkeys and all together our results demonstrate that SCS-induced
346 sensations obey a robust encoding scheme in the brain. Additionally, our behavioral experiments
347 serve as a test bed for future animal studies which could elucidate the neural mechanisms
348 underlying SCS-based sensory detection and discrimination. We envision that SCS can be
349 developed as an artificial sensory feedback channel for delivering targeted tactile and
350 proprioceptive information to the brain.

351

352 **Methods**

353 All animal procedures were approved by the Duke University Institutional Animal Care and Use
354 Committee and in accordance with National Institute of Health Guide for the Care and Use of
355 Laboratory Animals. Three adult rhesus macaque monkeys (Macaca mulatta), monkeys ‘M’, ‘O’,
356 and ‘K’ and Long Evans rats (300 - 350 g) participated in the experiments.

357 *Monkey spinal implant surgery*

358 Monkeys M, K, and O were implanted with 8-contact cylindrical percutaneous leads (Model 3186,
359 diameter 1.4mm, contact length 3 mm, spacing 4 mm, Abbott Laboratories) bilaterally to the spinal
360 mid-line in the dorsal epidural space at T6 – T8 spinal level. Monkey M had two leads with 8
361 stimulation contacts each, monkey O had two leads, one with 8 contacts (right side) and one with
362 4 contacts (left side, Model 3146, similar electrode contact dimensions as Model 3186), and
363 monkey K had two leads with 8 stimulation contacts each. Experimental procedures for monkeys
364 M, O, and K lasted approximately 45, 135, and 150 days post-implant after which the leads were
365 explanted (Supplementary Figure 1a).

366 Implant surgery was performed under general anesthesia using standard procedures typical of
367 human implantation (for details see supplementary information and Supplementary Figures 1b
368 and 1c). Once leads were implanted in the epidural space, a small hole was created in the skin
369 off-midline to externalize the distal end of the lead. Externalized leads were enclosed in a custom
370 plastic cap which was sutured to the skin (Supplementary Figure 1d). The plastic cap allowed for
371 access to the leads by the researcher but protection from the animal. The animal wore a protective
372 vest after surgery and throughout the experimental period which prevented its access to the
373 plastic cap sutures to its back.

374 *Monkey SCS detection task*

375 Monkeys were trained to perform a two-alternative forced choice task where they were seated in
376 a chair facing a computer monitor which indicated trial progression (Figure 1b). On each trial a
377 center target appeared, and the monkey had to move a cursor which was joystick-controlled inside
378 the center target (Figure 1c). After a brief hold period of 500 milliseconds (ms) inside the center
379 target, two targets appeared on either side of the center target. Each monkey had to hold the
380 cursor inside the central target for a brief period of 500 ms – 1 second. During this hold period
381 movement cues were presented. If SCS was presented (charge-balanced, cathode-first, 200 μs
382 biphasic square pulses at 100 Hz for 1 second using custom microstimulator (32)), then the

monkey had to move the cursor to the left target to obtain a juice reward. If SCS was absent, then the monkey had to move the cursor inside the right target. At the end of the hold period, the center target disappeared, thus cuing the monkey to initiate cursor movement toward the reward. Incorrect target reaches were not rewarded. Initiation of movement prior to the end of the hold period terminated the trial without reward and a blank screen was displayed 3 seconds before starting next trial. The learning performance of monkeys was studied using percentage correct (PC) trials.

*Monkey psychometric evaluation of detection thresholds*

Once monkeys were trained on the detection task, detection thresholds were determined for different electrode combinations using psychometric testing. Particularly, during 'Stimulation ON' i.e. 'left target rewarded' trials, the stimulation amplitude was randomly varied from 50 μA to a manually determined upper limit which was below the motor threshold. Only left target trials were analyzed and a percentage correct (PC) performance at each stimulation amplitude value was determined. A sigmoid curve was fit to the PC values and 75% was considered as detection threshold. This was repeated for several electrode combinations.

*Monkey electrode mapping*

In monkey K, once sensory detection thresholds were determined, we mapped the location of electrode pairs to location on the monkey's body by sedating the monkey and stimulating those electrodes above the sensory threshold values. Areas on the body surface that elicited minor muscle twitches or skin flutter were marked (Figure 2c, left) and the motor thresholds were noted. In monkey O, these observations were not made under sedation but while it was seated in the primate chair.

*Monkey detection thresholds as stimulation parameters vary*

406 During sets of consecutive sessions, we varied amplitude and frequency or amplitude and pulse-
407 width or amplitude and duration of stimulation while keeping other parameters constant (for
408 stimulation parameter ranges, see Supplementary Table 1). The standard parameters that
409 remained constant while others were varied were frequency: 100 Hz, pulse width: 200 μsec, and
410 duration: 1 sec. In monkey K, we varied frequency (10 – 1000 Hz) and duration (1 – 2000 ms) of
411 stimulation simultaneously while keeping pulse width and amplitude constant at 200 μs and 325
412 μA respectively. Detection thresholds for each monkey were normalized by maximum amplitude
413 used in the experiment block of that monkey before statistical analysis.

414 *Monkey sensory discrimination*

415 In the frequency discrimination task, each monkey was instructed to move the cursor inside the
416 left target for 100 Hz and right target for 200 Hz respectively (Figure 6a). In the spatial
417 discrimination task, the monkey was instructed to move the cursor inside the left target for
418 electrode pair 1 and inside right target for electrode pair 2 respectively (Figure 6c).

419 *Rat pre-training and SCS electrode implantation*

420 Moderately water deprived rats were placed inside the behavioral chamber for 2 days to
421 acclimatize to the behavioral environment. The behavioral chamber had two doors on one side of
422 the walls which enclosed water reward ports (Figure 4a), slightly modified from the one previously
423 described (33). Rats were gradually trained to receive water reward from the ports. Initially, both
424 reward doors were kept open and rats learned to receive water by licking at the water dispensing
425 spout. Later, the doors were kept closed and would open a few seconds after the house light
426 turned on. In subsequent sessions, left and right doors would open on alternate trials and rats
427 learned to obtain reward from each port alternatively. The pre-surgical training period lasted
428 approximately 8-10 days.

429 Thereafter custom designed SCS electrodes (1 mm X 0.5 mm contacts arranged transversely in
430 a bipolar configuration with 0.25 mm spacing using a 0.025mm thickness platinum foil, Goodfellow
431 Cambridge Limited, England) were implanted into the epidural space under T3 vertebra as
432 described in our previous article (29). After the rats recovered from the spinal surgical procedures,
433 cathode leading stimulation pulse trains were delivered at the SCS electrodes using a multi-
434 channel constant current stimulator (Master-8, A.M.P.I, Jerusalem, Israel) at stimulation settings
435 which were determined depending on the behavioral task under consideration (Figure 4a).

436 *Rat sensory detection task*

437 After recovery from surgery, rats were introduced to a two-alternative forced choice task (2AFC)
438 to learn detection of SCS stimuli in the chamber (Figure 4b). At the beginning of each trial, a light
439 in the chamber was turned on for 1 second as a reminder for the animals to pay attention. After
440 the light turned off, the rats received a sensory cue for 1 second. The sensory cue either consisted
441 of cathode-leading bipolar square pulse trains (pulse width: 200 μs, Frequency: 100 Hz, duration:
442 1 s) or no stimulation pulses (interval: 1 s) at each trial. After a brief delay of 0.5 seconds both
443 reward doors opened, and rats had to respond by choosing the left door for 'SCS ON' trials and
444 right door for 'SCS OFF' trials. Incorrect responses were not rewarded. During the learning of this
445 basic detection task, the intensity of the delivered current was determined before each session
446 and set using procedures described before (14, 29, 31) (mean±std, intensity at 100 Hz was 243.7
447 ± 57.9 μA).

448 *Rat sensory detection psychophysics*

449 Once rats learned the basic sensory detection task and their performance was above 80%,
450 stimulation parameters were varied in a systematic manner during the SCS-ON trials. In different
451 experimental sessions, stimulation parameters such as frequency and amplitude, pulse-width and
452 amplitude, and pulse train duration and amplitude were varied while other parameters were kept

453 constant (standard parameters: pulse width: 200 μs; Frequency: 100 Hz; duration: 1 s), and
454 sensory detection threshold amplitude was determined (for stimulation parameter ranges see
455 Supplementary Table 1). For all the conditions, the detectable level of the amplitude was defined
456 as 75% accuracy of behavioral performance. Detection thresholds for each rat were normalized
457 by maximum amplitude used in the experiment block of that rat before statistical analysis.

458 *Rat sensory discrimination task*

459 In a 2AFC task, rats were presented with either a low frequency stimulus or a high frequency
460 stimulus during the sensory cue period in the behavioral chamber. For either frequency, the
461 stimulus was delivered at the same amplitude (determined at each session), pulse width (200 μs),
462 and duration (1 sec). After a brief delay period following sensory cue presentation, rats had to
463 choose the left door for higher frequency stimulus and right door for lower frequency stimulus to
464 obtain reward (Supplementary Figure 4a). Initially, rats were trained to discriminate between 10
465 Hz and 100 Hz frequency. Incorrect trails were not rewarded.

466 *Weber's law and sensory discrimination*

467 Once rats learned to discriminate 10 Hz stimulus from 100 Hz stimulus, demonstrated by
468 consistent discrimination performance above 80%, the lower frequency (standard frequency) was
469 kept constant during right door trials while the higher frequency (comparison frequency) was
470 randomized between 20 Hz and 110 Hz during left door trials. Sensory discrimination performance
471 between a standard frequency and comparison frequency was determined as the fraction of trials
472 successfully discriminated for that particular standard and comparison pair. Thus, fraction trials
473 discriminated was plotted as a function of comparison frequency to obtain Just-Noticeable
474 Differences (JNDs) determined as 75 % value on the curve. The same experiment was repeated
475 for different standard frequency values such as 20 Hz vs (40 – 220 Hz), 40 Hz vs (60 – 240 Hz),

60 Hz vs (85 – 310 Hz), 80 Hz vs (110 – 380 Hz), and 100 Hz vs (130 – 400 Hz) to obtain JNDs for each standard frequency value and to test for Weber's law.

Similarly, the experiment was repeated for discrimination of a low-frequency comparison stimulus from a high-frequency standard stimulus. The standard frequency values were 110, 220, 310, 380, and 400 Hz, while the comparison frequency was randomized from (100 – 10 Hz), (200 – 20 Hz), (285 – 60 Hz), (350 – 80 Hz), and (370 – 100 Hz) respectively for each of the standard frequency values. JNDs were calculated for each of the standard frequency values as explained before to test for Weber's law.

*Statistical Analysis*

Repeated measures one-way ANOVA was used to test the significance of relationship between stimulation parameters and sensory detection thresholds in both rats and monkeys (Figures 3h, 3i, 3j, 5g, 5h, and 5i). To test whether JNDs were significantly linearly related to standard frequency in the sensory discrimination task, the linear regression test was used (Figures 7b and 7d).

502 **References**

503 1. Lebedev MA, Nicolelis MA. Brain-Machine Interfaces: From Basic Science to Neuroprostheses and
504 Neurorehabilitation. Physiol Rev. 2017;97(2):767-837. doi: 10.1152/physrev.00027.2016. PubMed PMID:
505 28275048.

506 2. Krucoff MO, Rahimpour S, Slutzky MW, Edgerton VR, Turner DA. Enhancing Nervous System
507 Recovery through Neurobiologics, Neural Interface Training, and Neurorehabilitation. Frontiers in
508 neuroscience. 2016;10. doi: ARTN 584

509 10.3389/fnins.2016.00584. PubMed PMID: WOS:000390598100001.

510 3. Bensmaia SJ, Miller LE. Restoring sensorimotor function through intracortical interfaces: progress
511 and looming challenges. Nat Rev Neurosci. 2014;15(5):313-25. doi: 10.1038/nrn3724. PubMed PMID:
512 24739786.

513 4. O'Doherty JE, Lebedev MA, Ifft PJ, Zhuang KZ, Shokur S, Bleuler H, Nicolelis MA. Active tactile
514 exploration using a brain-machine-brain interface. Nature. 2011;479(7372):228-31. doi:
515 10.1038/nature10489. PubMed PMID: 21976021; PMCID: 3236080.

516 5. Kim S, Callier T, Tabot GA, Gaunt RA, Tenore FV, Bensmaia SJ. Behavioral assessment of sensitivity
517 to intracortical microstimulation of primate somatosensory cortex. Proceedings of the National Academy
518 of Sciences of the United States of America. 2015;112(49):15202-7. doi: 10.1073/pnas.1509265112.
519 PubMed PMID: 26504211; PMCID: 4679002.

520 6. Tabot GA, Dammann JF, Berg JA, Tenore FV, Boback JL, Vogelstein RJ, Bensmaia SJ. Restoring the
521 sense of touch with a prosthetic hand through a brain interface. P Natl Acad Sci USA. 2013;110(45):18279-
522 84. doi: 10.1073/pnas.1221113110. PubMed PMID: WOS:000326550800062.

523 7. Flesher SN, Collinger JL, Foldes ST, Weiss JM, Downey JE, Tyler-Kabara EC, Bensmaia SJ, Schwartz
524 AB, Boninger ML, Gaunt RA. Intracortical microstimulation of human somatosensory cortex. Science
525 translational medicine. 2016;8(361):361ra141. Epub 2016/11/01. doi: 10.1126/scitranslmed.aaf8083.
526 PubMed PMID: 27738096.

527 8. Heming E, Sanden A, Kiss ZH. Designing a somatosensory neural prosthesis: percepts evoked by
528 different patterns of thalamic stimulation. Journal of neural engineering. 2010;7(6):064001. doi:
529 10.1088/1741-2560/7/6/064001. PubMed PMID: 21084731.

530 9. Swan BD, Gasperson LB, Krucoff MO, Grill WM, Turner DA. Sensory percepts induced by microwire
531 array and DBS microstimulation in human sensory thalamus. Brain Stimul. 2018;11(2):416-22. doi:
532 10.1016/j.brs.2017.10.017. PubMed PMID: 29126946; PMCID: PMC5803348.

533 10. Dadarlat MC, O'Doherty JE, Sabes PN. A learning-based approach to artificial sensory feedback
534 leads to optimal integration. Nature neuroscience. 2015;18(1):138-44. Epub 2014/11/25. doi:
535 10.1038/nn.3883. PubMed PMID: 25420067; PMCID: PMC4282864.

536 11. Strauss I, Valle G, Artoni F, D'Anna E, Granata G, Di Iorio R, Guiraud D, Stieglitz T, Rossini PM,
537 Raspopovic S, Petrini FM, Micera S. Characterization of multi-channel intraneural stimulation in
538 transradial amputees. Sci Rep. 2019;9(1):19258. Epub 2019/12/19. doi: 10.1038/s41598-019-55591-z.
539 PubMed PMID: 31848384; PMCID: PMC6917705.

540 12. Petrini FM, Valle G, Bumbasirevic M, Barberi F, Bortolotti D, Cvancara P, Hiairrassary A, Mijovic P,
541 Sverrisson AO, Pedrocchi A, Divoux JL, Popovic I, Lechler K, Mijovic B, Guiraud D, Stieglitz T, Alexandersson
542 A, Micera S, Lesic A, Raspopovic S. Enhancing functional abilities and cognitive integration of the lower
543 limb prosthesis. Science translational medicine. 2019;11(512). Epub 2019/10/04. doi:
544 10.1126/scitranslmed.aav8939. PubMed PMID: 31578244.

545 13. Petrini FM, Bumbasirevic M, Valle G, Ilic V, Mijovic P, Cvancara P, Barberi F, Katic N, Bortolotti D,
546 Andreu D, Lechler K, Lesic A, Mazic S, Mijovic B, Guiraud D, Stieglitz T, Alexandersson A, Micera S,
547 Raspopovic S. Sensory feedback restoration in leg amputees improves walking speed, metabolic cost and
548 phantom pain. Nat Med. 2019;25(9):1356-63. Epub 2019/09/11. doi: 10.1038/s41591-019-0567-3.
549 PubMed PMID: 31501600.

550 14. Yadav AP, Li D, Nicolelis MAL. A Brain to Spine Interface for Transferring Artificial Sensory
551 Information. Sci Rep. 2020;10(1):900. Epub 2020/01/23. doi: 10.1038/s41598-020-57617-3. PubMed
552 PMID: 31964948.

553 15. Bellanca RU, Lee GH, Vogel K, Ahrens J, Kroeker R, Thom JP, Worlein JM. A simple alopecia scoring
554 system for use in colony management of laboratory-housed primates. J Med Primatol. 2014;43(3):153-61.
555 Epub 2014/02/28. doi: 10.1111/jmp.12107. PubMed PMID: 24571509; PMCID: PMC4438708.

556 16. Ekman G. Weber Law and Related Functions. Journal of Psychology. 1959;47(2):343-52. doi: Doi
557 10.1080/00223980.1959.9916336. PubMed PMID: WOS:A1959CAK1200020.

558 17. Bjanes DA, Moritz CT. A Robust Encoding Scheme for Delivering Artificial Sensory Information via
559 Direct Brain Stimulation. IEEE Trans Neural Syst Rehabil Eng. 2019;27(10):1994-2004. Epub 2019/08/24.
560 doi: 10.1109/TNSRE.2019.2936739. PubMed PMID: 31443035.

561 18. Merrill DR, Bikson M, Jefferys JG. Electrical stimulation of excitable tissue: design of efficacious
562 and safe protocols. J Neurosci Methods. 2005;141(2):171-98. Epub 2005/01/22. doi:
563 10.1016/j.jneumeth.2004.10.020. PubMed PMID: 15661300.

564 19. Cogan SF, Ludwig KA, Welle CG, Takmakov P. Tissue damage thresholds during therapeutic
565 electrical stimulation. Journal of neural engineering. 2016;13(2):021001. Epub 2016/01/23. doi:
566 10.1088/1741-2560/13/2/021001. PubMed PMID: 26792176; PMCID: PMC5386002.

567 20. Romo R, Hernandez A, Zainos A, Brody CD, Lemus L. Sensing without touching: psychophysical
568 performance based on cortical microstimulation. Neuron. 2000;26(1):273-8. PubMed PMID: 10798410.

569 21. O'Doherty JE, Shokur S, Medina LE, Lebedev MA, Nicolelis MAL. Creating a neuroprosthesis for
570 active tactile exploration of textures. Proceedings of the National Academy of Sciences of the United
571 States of America. 2019;116(43):21821-7. Epub 2019/10/09. doi: 10.1073/pnas.1908008116. PubMed
572 PMID: 31591224; PMCID: PMC6815176.

573 22. Callier T, Brantly NW, Caravelli A, Bensmaia SJ. The frequency of cortical microstimulation shapes
574 artificial touch. Proceedings of the National Academy of Sciences of the United States of America.
575 2020;117(2):1191-200. Epub 2019/12/28. doi: 10.1073/pnas.1916453117. PubMed PMID: 31879342;
576 PMCID: PMC6969512.

577 23. Holsheimer J, Barolat G. Spinal geometry and paresthesia coverage in spinal cord stimulation.
578 Neuromodulation : journal of the International Neuromodulation Society. 1998;1(3):129-36. doi:
579 10.1111/j.1525-1403.1998.tb00006.x. PubMed PMID: 22150980.

580 24. Barolat G, Massaro F, He J, Zeme S, Ketcik B. Mapping of sensory responses to epidural stimulation
581 of the intraspinal neural structures in man. Journal of neurosurgery. 1993;78(2):233-9. Epub 1993/02/01.
582 doi: 10.3171/jns.1993.78.2.0233. PubMed PMID: 8421206.

583 25. Holsheimer J, Buitenweg JR. Review: Bioelectrical mechanisms in spinal cord stimulation.
584 Neuromodulation : journal of the International Neuromodulation Society. 2015;18(3):161-70; discussion
585 70. doi: 10.1111/ner.12279. PubMed PMID: 25832787.

586 26. North RB, Sieracki JM, Fowler KR, Alvarez B, Cutchis PN. Patient-interactive, microprocessor-
587 controlled neurological stimulation system. Neuromodulation : journal of the International
588 Neuromodulation Society. 1998;1(4):185-93. Epub 1998/10/01. doi: 10.1111/j.1525-
589 1403.1998.tb00015.x. PubMed PMID: 22151030.

590 27. Holsheimer J. Which Neuronal Elements are Activated Directly by Spinal Cord Stimulation.
591 Neuromodulation : journal of the International Neuromodulation Society. 2002;5(1):25-31. Epub
592 2002/01/01. doi: 10.1046/j.1525-1403.2002._2005.x. PubMed PMID: 22151778.

593 28. Yadav AP, Nicolelis MAL. Electrical stimulation of the dorsal columns of the spinal cord for
594 Parkinson's disease. Mov Disord. 2017;32(6):820-32. doi: 10.1002/mds.27033. PubMed PMID: 28497877.

595 29. Yadav AP, Fuentes R, Zhang H, Vinholo T, Wang CH, Freire MA, Nicolelis MA. Chronic spinal cord
596 electrical stimulation protects against 6-hydroxydopamine lesions. Sci Rep. 2014;4:3839. doi:
597 10.1038/srep03839. PubMed PMID: 24452435; PMCID: 3899601.

598 30. Yadav AP, Borda E, Nicolelis MA. Closed loop spinal cord stimulation restores locomotion and
599 desynchronizes corticostriatal beta oscillations [abstract]. Mov Disord. 2018;33.

600 31. Pais-Vieira M, Yadav AP, Moreira D, Guggenmos D, Santos A, Lebedev M, Nicolelis MA. A Closed
601 Loop Brain-machine Interface for Epilepsy Control Using Dorsal Column Electrical Stimulation. Sci Rep.
602 2016;6:32814. doi: 10.1038/srep32814. PubMed PMID: 27605389; PMCID: PMC5015048.

603 32. Hanson TL, Omarsson B, O'Doherty JE, Peikon ID, Lebedev MA, Nicolelis MA. High-side digitally
604 current controlled biphasic bipolar microstimulator. IEEE Trans Neural Syst Rehabil Eng. 2012;20(3):331-
605 40. Epub 2012/02/14. doi: 10.1109/TNSRE.2012.2187219. PubMed PMID: 22328184; PMCID:
606 PMC3502026.

607 33. Pais-Vieira M, Chiuffa G, Lebedev M, Yadav A, Nicolelis MA. Building an organic computing device
608 with multiple interconnected brains. Sci Rep. 2015;5:11869. doi: 10.1038/srep11869. PubMed PMID:
609 26158615; PMCID: 4497302.

610 34. Krucoff MO, Zhuang K, MacLeod D, Yin A, Byun YW, Manson RJ, Turner DA, Oliveira L, Lebedev
611 MA. A novel paraplegia model in awake behaving macaques. Journal of neurophysiology.
612 2017;118(3):1800-8. Epub 2017/07/14. doi: 10.1152/jn.00327.2017. PubMed PMID: 28701540; PMCID:
613 PMC5596146.

614

615
616
617
618
619
620
621
622
623
624
625
626
627

## Acknowledgements

We thank Gary Lehew for assistance with experimental setup, Tamara Phillips for assistance with monkey handling, Paul Thompson for assistance with primate task software, Laura Oliveira and Susan Halkiotis for technical assistance, and Joseph O'Doherty for comments on previous version of manuscript. This research was supported by Duke Institute for Brain Sciences Germinator Award and Duke Neurosurgery Research Support offered to Amol Yadav, NIH R25 awarded to Max Krucoff, and Hartwell Foundation grant awarded to Miguel Nicolelis.

## Author Contributions

A.P.Y., S.L., M.O.K., and M.A.L, designed experiments, A.P.Y. and S.L. performed rodent experiments and surgeries, M.O.K and M.M.A performed primate surgeries, A.P.Y performed primate experiments, A.P.Y. and S.L. analyzed data, A.P.Y. drafted manuscript, all authors edited manuscript, M.A.L.N. supervised work.

## Competing financial interests

The authors declare no competing financial or non-financial interests

645 **Supplementary Information and Figures**

646 Primate implant surgery and timeline

647 Two weeks prior to surgery, the animal was acclimated to a protective vest. One day before
648 surgery, the animal's back was shaved with an electrical clipper under mild sedation. The day of
649 surgery, the animal underwent general anesthesia and endotracheal tube placement by staff
650 veterinarians. The animal was then positioned prone on a radiolucent fluoroscopy table. The spine
651 was placed into gentle flexion to open the interspinous spaces by placing the knees and pillows
652 under the abdomen of the monkey. Pressure points were carefully padded. The surgical area was
653 cleaned and prepped with 2% chlorhexidine gluconate and 70% isopropyl alcohol solution
654 (ChloraPrepTM) and allowed to dry for 3 minutes. The surgical area was then draped in a sterile
655 fashion. A dose of antibiotics was given within one hour prior to incision.

656 An anterior-posterior (AP) C-arm fluoroscopic x-ray was then taken to mark the level of the lowest
657 rib, and the radiographic shadows of the spinous processes were positioned in the middle of the
658 pedicles to ensure minimal rotation. After injecting a local anesthetic (1.5% lidocaine with
659 1:100,000 epinephrine), a 2cm incision was made at this location down to the fascia, and a self-
660 retaining retractor was placed to hold the skin open. A trocar was then introduced through the
661 fascia just lateral to midline between the spinous processes and advanced so the tip just entered
662 the epidural space. Epidural location was confirmed using a loss of resistance technique,
663 fluoroscopic x-ray, and lack of cerebrospinal fluid (CSF) (34). Next, an 8-contact cylindrical
664 percutaneous lead was introduced through the trocar and steered through dorsal epidural space
665 to a target location in the mid-thoracic spine, or approximately across T8 (Supplementary Figure
666 1b). Once in a satisfactory position, the stylet and trocar were removed. The lead was then
667 secured to the fascia using a 2-0 silk suture, and then a subcutaneous suprafascial pocket was
668 created off midline to secure lead excess. A small hole was then created in the skin off midline to
669 externalize the distal end of the lead. The same procedure was then repeated on the opposite

site, ultimately positioning the electrodes next to one another in the midline dorsal epidural thoracic space with a slight cranio-caudal offset (Supplementary Figure 1c).

Once both electrodes were externalized, the incision was closed with inverted dermal vicryl sutures and a running 4-0 nylon suture. The incision was then covered with a thin layer of bacitracin ointment, and piece of telfa was then placed over the incision and stapled to the skin. Next, a custom plastic cap was sutured to the animal's skin with 3-0 nylon sutures to cover the externalized leads (Supplementary Figure 1d). Such a cap allowed for access to the leads by the researcher but protection from the animal. The telfa was removed 3 days after surgery. Surgical sutures were removed 7-10 days after surgery. The sutures in the cap needed to be replaced approximately monthly under sedation.

Monkey M's right lead stopped working a few days post-implant while the left lead stopped working approximately 45 days post-implant. Hence the leads were explanted thereafter. Monkey O's left lead stopped working a few days post-implant while the right lead worked for 135 days after which they were extracted due to a skin infection at the externalization site. Monkey K's both left and right leads were working until they were explanted approximately 150 days after surgery due to a skin erosion at externalization site.

**Supplementary Figure 1**

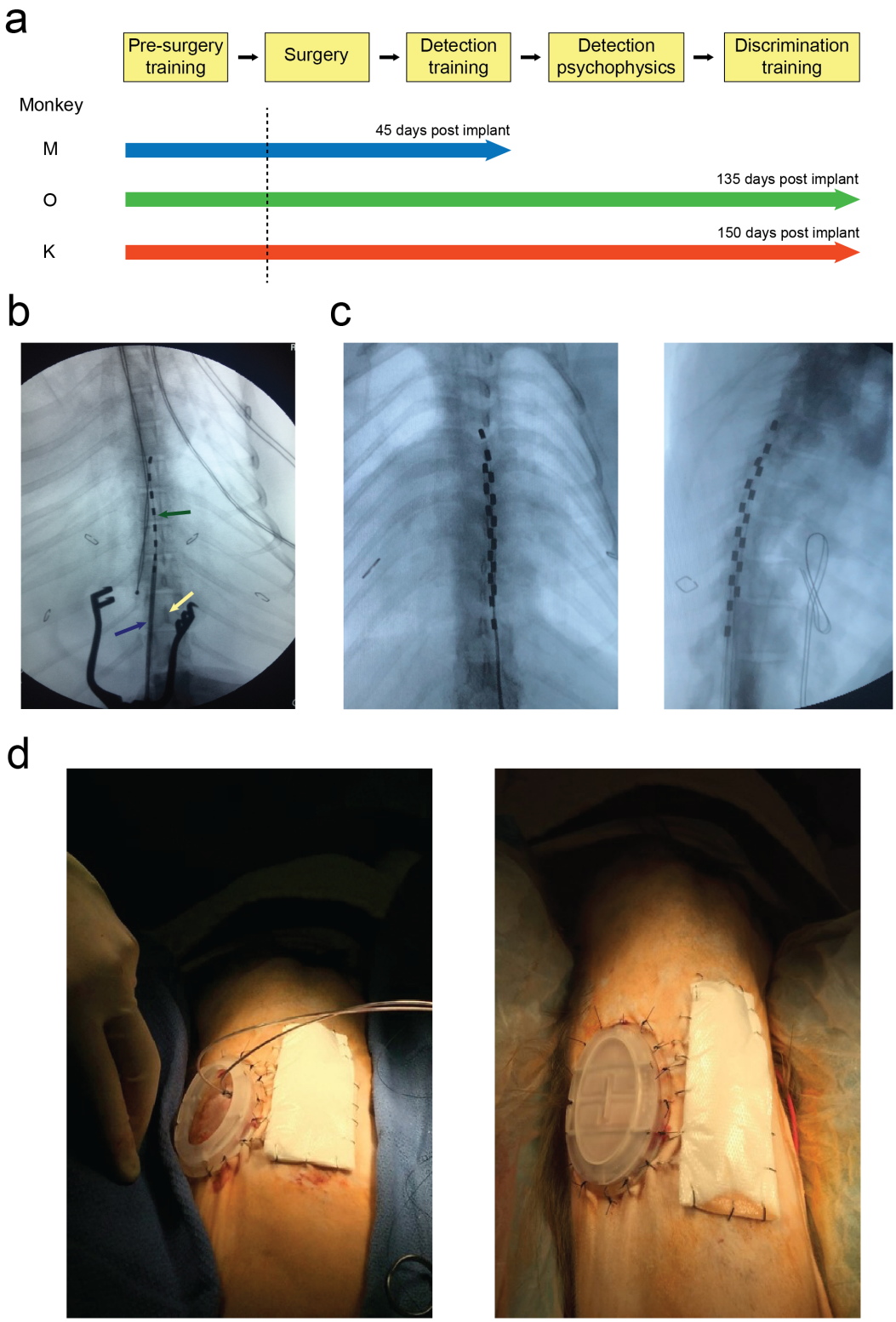

Supplementary Figure 1: Timeline of primate experiments and primate surgery procedures.

a) Monkeys were trained on the joystick task prior to spinal implant surgery. After they recovered from the surgery behavioral training began for detection of SCS-based sensations. After that sensory detection psychophysical experiments were performed followed by training on discrimination of SCS-based sensations. Monkey M learned the SCS detection task, however, 45 days after surgery its implanted spinal electrodes stopped working and hence were explanted. Spinal implants of Monkey O and K lasted until they both were trained on the SCS sensory discrimination task. However, 135 and 150 days after surgery for both monkeys the implants stopped working and were subsequently explanted. b) Anterior-posterior (AP) fluoroscopic x-ray showing the introduction of the 8-contact cylindrical lead through the trocar into the mid-thoracic dorsal epidural space. Blue arrow: trocar, Green arrow: 8-contact electrode array, Orange arrow: spinous process. c) Final AP (left) and lateral (right) x-rays showing placement of dorsal mid-thoracic epidural electrodes with slight cranio-caudal offset. d) Externalized electrodes with custom plastic cap sutured to the skin, and incision temporarily covered with telfa stapled to the skin. Cap open (left), cap closed (right).

718 **Supplementary Figure 2:**

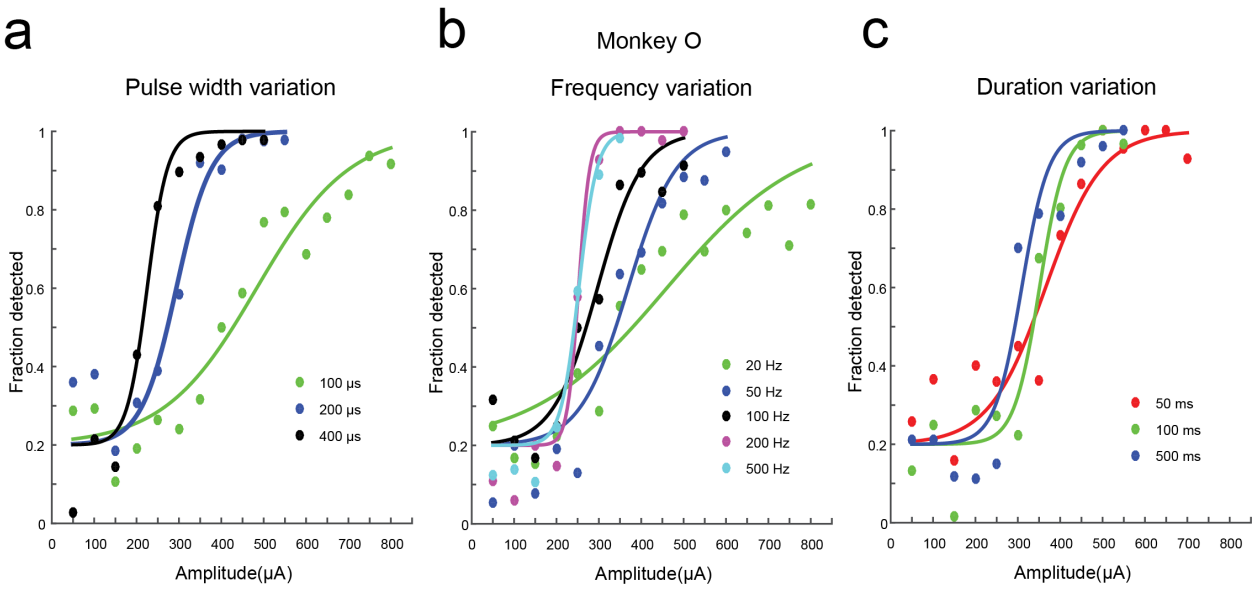


719

720 Supplementary Figure 2: Psychophysical evaluation of SCS sensory detection in monkey 'O' with varying
721 stimulation parameters. Once monkey O learned to detect SCS stimuli at the standard parameters
722 (frequency: 100 Hz, pulse width: 200 μs, duration: 1 sec), we allocated different blocks of sessions where
723 (pulse width & amplitude; panel 'a' ); (frequency & amplitude; panel 'b'); and (duration & amplitude; panel
724 'c') were varied while keeping other parameters constant. Psychometric curves in a-c are sigmoidal fits to
725 fraction of trials that were successfully detected as a function of amplitude.

726

727

728

729

730

731

732

**Supplementary Figure 3**

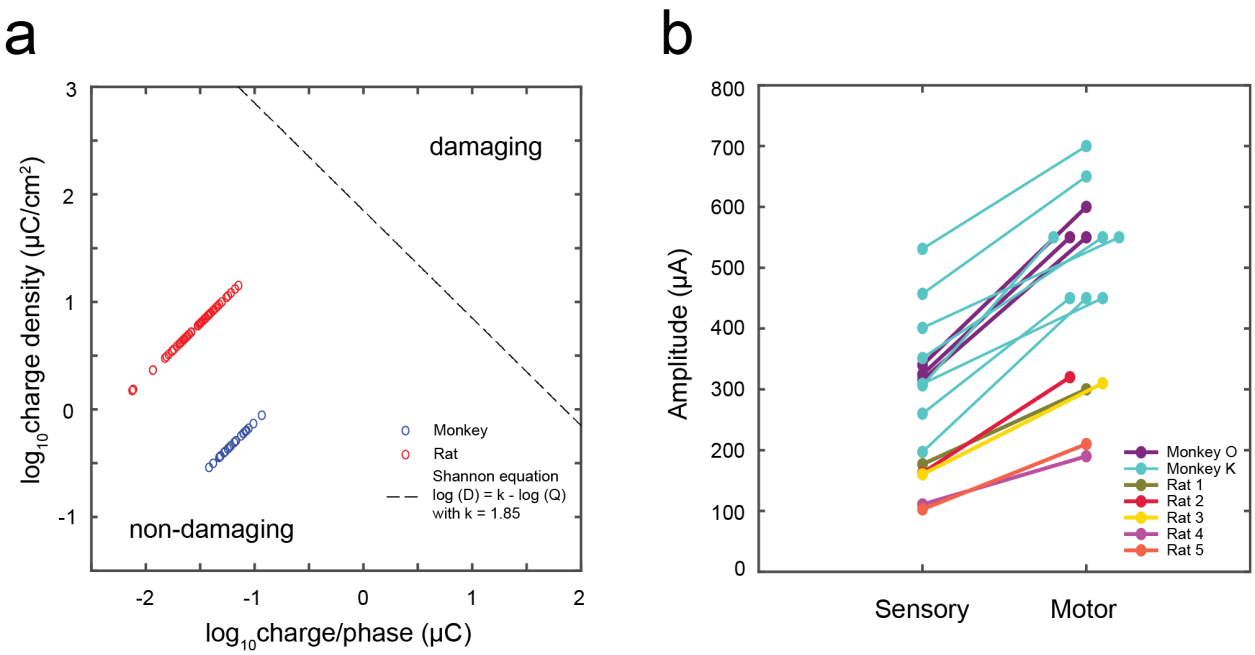


Supplementary Figure 3: Charge versus charge density and sensory versus motor thresholds. a) Sensory thresholds for monkeys (blue circles) and rats (red circles) determined by psychophysical evaluation at multiple stimulation parameters of pulse-width, frequency, and duration were below tissue damaging levels. Black dotted line indicates boundary between damaging and non-damaging stimulation defined by k = 1.85 in the Shannon equation [log(D) = k – log (Q)] on a log charge density (D) versus log charge per phase (Q) plot. b) Sensory thresholds were considerably lower than the amplitude levels where muscle twitches or skin fluctuations were observed on the animals' body. Purple and turquoise circles represent multiple electrode pairs tested in monkeys O and K respectively.

748 **Supplementary Figure 4**

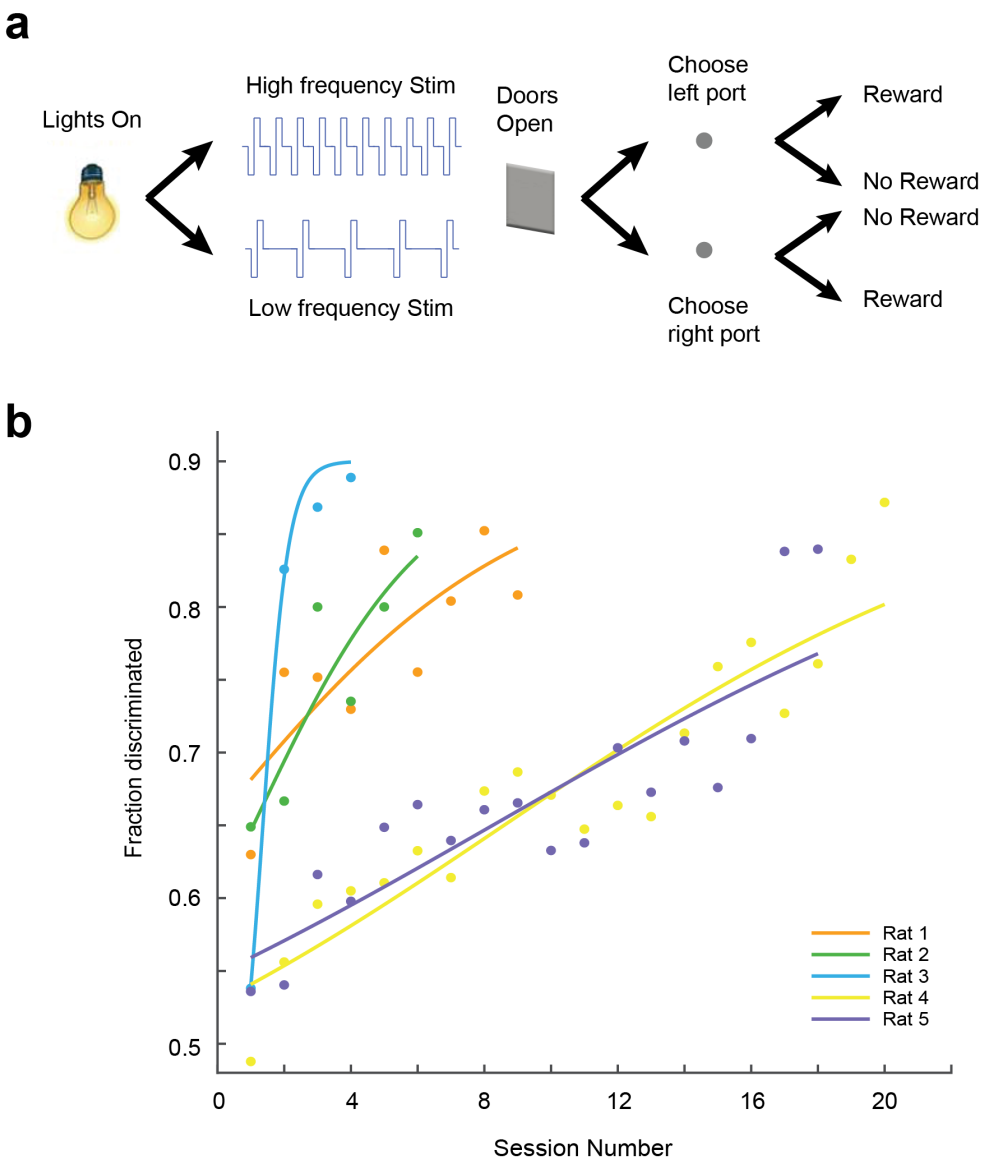


749

750 Supplementary Figure 4: Rats learned to discriminate SCS stimuli varying in frequency. a) Behavioral setup
751 for frequency discrimination task. Rats had to choose left reward port for higher frequency of SCS and right
752 reward port for lower frequency of stimulation. Stimulation was delivered at a constant amplitude at the
753 standard parameters (pulse width: 200 μs, duration: 1 sec) and rats had to choose the correct reward port
754 associated with each frequency to obtain water reward. b) Learning curves for five rats that learned to
755 discriminate two frequencies (10 Hz vs 100 Hz). Curves indicate sigmoidal fits to fraction of trials that were
756 successfully discriminated as a function of session number.

757 **Supplementary Table 1**

| Animal | Amplitude | Pulse Width | Frequency | Duration |
|---|---|---|---|---|
| Monkey O | 50 – 800 μA, 50 μA step | 100 – 400 μs | 20 – 500 Hz | 50 – 500 ms |
| Monkey K | 50 – 800 μA, 50 μA step | 50 – 400 μs | 10 – 500 Hz | 50 – 1000 ms |
| Rat 1 | 50 – 325 μA, 25 μA step | 50 – 400 μs | 10 – 500 Hz | 50 – 1000 ms |
| Rat 2 | 50 – 325 μA, 25 μA step | 50 – 400 μs | 10 – 500 Hz | 50 – 1000 ms |
| Rat 3 | 50 – 325 μA, 25 μA step | 50 – 400 μs | 10 – 500 Hz | 50 – 1000 ms |
| Rat 4 | 50 – 187.5 μA, 12.5 μA step | 50 – 400 μs | 10 – 500 Hz | 50 – 1000 ms |
| Rat 5 | 50 – 175 μA, 12.5 μA step | 50 – 400 μs | 10 – 500 Hz | 50 – 1000 ms |

758

759 Supplementary Table 1: Stimulation parameter ranges tested at psychophysical evaluation of
760 sensory detection. Animals were initially trained to detect SCS stimuli at standard stimulation
761 parameters – frequency: 100 Hz, pulse-width: 200 μs, and duration: 1000 ms) as shown in Figures
762 2a and 4c. After that sensory thresholds were determined by using stimulation settings shown
763 above. In blocks of consecutive sessions, amplitude and frequency or amplitude and pulse-width
764 or amplitude and duration of stimulation were varied while keeping other parameters constant. In
765 additional block of sessions in monkey K, frequency (10 – 1000 Hz) and duration (1 – 2000 ms)
766 of stimulation were simultaneously varied while keeping pulse width and amplitude constant at
767 200 μs and 325 μA respectively.